Superlattice formation in titanium diselenide*

K. C. Woo, F. C. Brown, W. L. McMillan, R. J. Miller, M. J. Schaffman, and M. P. Sears
Department of Physics and Materials Research Laboratory, University of Illinois, Urbana, Illinois 61801
(Received 22 December 1975)

Experimental results are presented on the interesting $2a_0$ by $2c_0$ superlattice which forms in $Ti_{1+x}Se_2$ at low temperature. A second-order phase transition has been found at $T_c \cong 150$°K in crystals grown by iodine vapor transport at ~ 800°C. This transition has been studied by electron and x-ray diffraction, magnetic susceptibility, resistivity, and infrared reflectivity. It appears to be a normal to lock-in transition with instability and strong diffuse scattering above T_c. It is suggested that the instability is Fermi-surface driven and that strong electron scattering occurs involving a zone-boundary phonon. A far-infrared lattice mode is observed which breaks up into several additional modes below the phase transition.

I. INTRODUCTION

The diverse physical properties of the transition-metal dichalcogenides are discussed in the widely cited review by Wilson and Joffe.[1] These highly anisotropic layer materials possess a wide range of electrical and optical properties including semiconducting, metallic, and superconducting behavior. The effect of intercalation on the superconducting transition temperature was studied for a number of years. More recently the discovery of charge-density waves in the group-V*b* compounds has motivated intensive investigations.[2] In this paper we report on superlattice formation in $TiSe_2$, a group-IV*b* dichalcogenide. Because charge-density waves are closely associated with the topology of the Fermi surface a knowledge of the electronic properties and band structure is crucial.

The group-IV*b* compounds TiS_2 and $TiSe_2$ exhibit metallic or semimetallic conductivity, unlike the corresponding zirconium and hafnium compounds which are semiconductors. This is at variance with published band-structure results[3] which indicate a 1 or 2-V gap between filled valence bands and empty *d*-like conduction bands. For example,[4] the maximum of the valence band in HfS_2 occurs at the center of the Brillouin zone and the minimum of the conduction band on the zone boundary at either *M* or *L*. Although the energy bands of TiS_2 are not quite two dimensional, a two-dimensional diagram is probably adequate to illustrate these general features. The solid curves in Fig. 1(a) are drawn after Myron and Freeman's[3] calculation and they indicate an indirect gap between Γ_3^- and M_1^+.

Departure from stoichiometry is a problem in TiS_2 and $TiSe_2$ and could account for the excess conductivity, the extra titanium entering between layers where it can conceivably donate electrons to the *d*-like conduction bands.[5] On the other hand, Thompson *et al.*[6] have given convincing evidence that stoichiometric TiS_2 can be prepared and that the material is still highly conducting both at room and at low temperature. Apparently *p*-*d* band overlap occurs creating holes at Γ and electrons at *M* in the Brillouin zone, therefore TiS_2 is a semi-

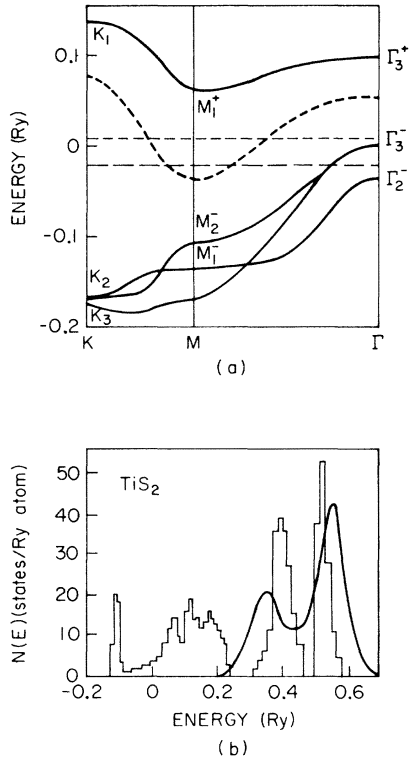

FIG. 1. (a) Energy-band structure for TiS_2 calculated by Myron and Freeman (Ref. 3). The dashed conduction band has been lowered so as to provide band overlap in line with recent experimental evidence. The horizontal dashed lines are Fermi levels for stoichiometric and for excess titanium crystals. (b) The smooth curve shows the sulfur L_{III} absorption spectrum of Sonntag and Brown (Ref. 7) superimposed on the density-of-states histogram for TiS_2 (Ref. 3).

metal. This is still consistent with soft-x-ray absorption measurements on TiS_2.[7] For example, Fig. 1(b) shows the observed sulfur L_{III} absorption curve superimposed upon the density-of-states histogram calculated by Myron and Freeman.[3] Notice that the two peaks (corresponding to t_{2g} and e_g molecular orbitals) are more widely spaced than theory and may overlap the valence band.[8]

Band overlap in $TiSe_2$ is even more likely than in TiS_2 because of less electronegativity difference of cation and anion. In fact, Bachrach *et al.*[9] have recently used the technique of angle-resolved photoemission to study the occupied density of state in nonstoichiometric $TiSe_2$. Their results show a band structure rather like that discussed above for TiS_2 but modified so that the conduction and valence bands overlap in k space. Conduction bands (two dimensional) shifted so as to allow for this overlap are shown by dashed lines in Fig. 1(a). In the slightly nonstoichiometric crystals studied by Bachrach *et al.* [(2–4)% excess titanium] no holes were detected at Γ_3^-, and it was found that the Fermi level lay just above Γ_3' as indicated by the upper horizontal dashed line in Fig. 1(a). In the present paper we report on a variety of experiments on similar crystals. These experiments include electron and x-ray diffraction, magnetic susceptibility, resistivity, and infrared reflectivity.

The growth and characterization of crystals, particularly as to stoichiometry, are crucial in these investigations. Clearly the close proximity and small overlap of d conduction bands and p-like bonding orbitals is very sensitive to composition, e.g., to the parameter x in the formula $Ti_{1+x}Se_2$. At the same time, it is quite difficult to determine x with the required accuracy. We have tried both electron microprobe and chemical (gravimetric) analysis. The exact composition of crystals grown by vapor transport depends upon growth temperature as well as other variables. In fact there may even be some small variation in composition for crystals from a given batch, grown in the same sealed tube. Most materials reported on to date are the result of growth in the range 800–900 °C where the yield is high and thin crystals of large area are relatively easily obtained. All of the crystals reported on here are of this type.

Several groups have reported a low-temperature transformation or distortion in $TiSe_2$. For example, Thompson[10] lists a transformation temperature $T_c \sim 200$ °K but does not discuss the nature of the transition. Wilson[11] has commented on the $2a_0$ superlattice which forms in $TiSe_2$ below T_c, and he has pointed out that the mechanism may be fundamentally different than charge-density waves in the group-Vb compounds. He speculates that coupled electrons and holes drive an instability in which a zone-boundary phonon takes part. An exciting possibility is that the so-called excitonic state[12] of matter may be involved. In Sec. II we show the results of electron and x-ray diffraction studies of the normal to lock-in transition which occurs at about 150 °K in the nonstoichiometric crystals investigated. Other measurements including infrared reflectivity are reported in Secs. II–IV and, by way of conclusion, some models are presented which help to explain the various results.

II. DIFFRACTION STUDIES OF THE SUPERLATTICE

The crystals of $Ti_{1+x}Se_2$, as well as mixed $TiSe_{2-x}S_x$ samples, were grown by iodine vapor transport in sealed quartz tubes according to the method of Schafer.[13] Carefully weighed amounts of titanium wire, sulfur, and selenium, of 99.999% purity were used as starting materials. Analysis by mass spectrometer indicated very small concentrations of Fe and other impurities (<10 ppm) and an iodine content in the final crystals $\lesssim 500$ ppm. Most of the $Ti_{1+x}Se_2$ samples were grown between 750 and 800 °C in tubes containing a slight excess of Se. The resulting crystals were excess in titanium but gravimetric analysis for both Ti and Se indicated that x was not greater than 0.02 in the formula $Ti_{1+x}Se_2$. Crystals were also grown in the temperature range 500–600 °C. Although such crystals are more stoichiometric they were not used in the present investigations.

Figure 2(a) shows a room-temperature transmission electron diffraction pattern for a thin cleaved crystal of $Ti_{1+x}Se_2$ containing a small excess ($x \sim 0.02$) of titanium. The pattern was taken on a JEOL 200-keV electron microscope. A hexagonal spot pattern characteristic of the CdI_2 layer structure (space group D_{3d}^3) is seen. In addition one notices a marked streaking and broad diffraction intensity halfway between the principal spots. This is seen in all $Ti_{1+x}Se_2$ crystals over a wide range of Ti excess as well as in $TiSe_{2-x}S_x$ crystals with nominal sulfur content as high as 75%. Apparently it is due to local fluctuations into the $2a_0$ superlattice. Fluctuations of this type may be enhanced by defects such as the excess titanium.

Figure 2(b) shows an electron diffraction pattern for the sample of Fig. 2(a) but cooled on a liquid-nitrogen stage to about 120 °K. This is well below the transition temperature $T_c \sim 150$ °K. Additional sharp spots of the $2a_0$ superlattice are seen. Notice that they occur midway ($\frac{1}{2}a_0^*$) between the normal hexagonal-reciprocal-lattice spots. Tilt experiments as well as x-ray diffraction studies indicate that the new low-temperature superlattice is actually of $2a_0$ by $2c_0$ periodicity. This is in

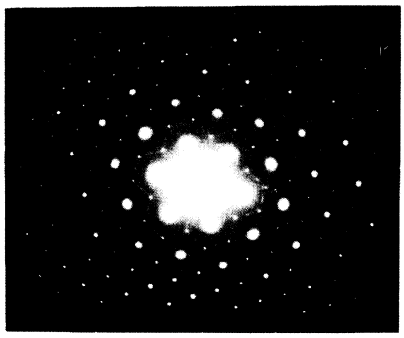

(a)

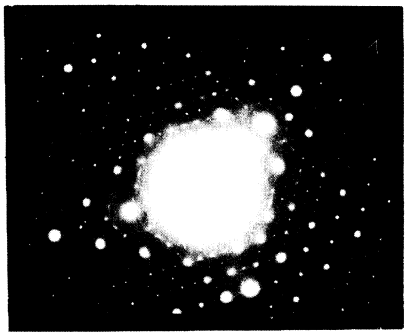

(b)

FIG. 2. (a) Electron diffraction pattern for a crystal of $Ti_{1+x}Se_2$ ($x \sim 0.02$) at room temperature. In addition to the normal hexagonal diffraction pattern diffuse streaking appears especially near the midpoints of the lines joining two spots. (b) A pattern for the same crystal at 120 °K which is below the lock-in transition. Note the sharp $\frac{1}{2}a_0^*$ spots.

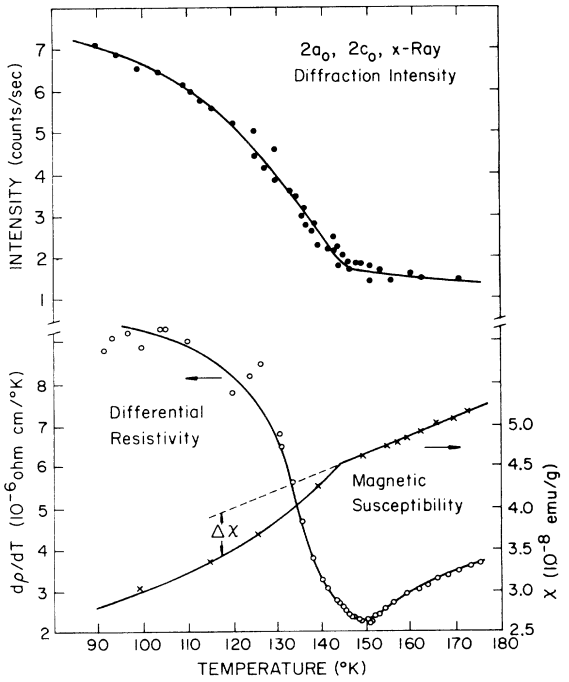

FIG. 3. Scattered x-ray intensity for the $\frac{1}{2}a_0^*$ spots as a function of temperature (upper). Differential resistivity and magnetic susceptibility vs temperature for $Ti_{1+x}Se_2$ (lower).

contrast to the *ABC* type stacking of the charge-density waves in $1T$-TaS_2 which achieves low electrostatic interaction between planes.[2] The patterns shown in Fig. 2 are characteristic of a majority of the crystals investigated. One sample was found, however, in which a slightly shortened $4a_0$ pattern was observed at low temperature in addition to the $(2a_0, 2c_0)$ superlattice.

X-ray diffraction studies were also carried out on these $Ti_{1+x}Se_2$ crystals. The results with copper $K\alpha$ radiation corroborate the electron diffraction evidence. The experimental arrangement included a LiF crystal monochromator in order to provide a collimated highly monochromatic beam of characteristic radiation. This beam was then incident on the $TiSe_2$ crystal mounted in a cryostat on an accurate diffractometer. Photon counting was employed. The intensity of Bragg scattering from the $(2a_0, 2c_0)$ superlattice is shown as a function of temperature from 80 to 170 °K in the top of Fig. 3. Notice that a transition sets in at $T_c = 150 \pm 5$ °K below which the intensity increases approximately as $1-(T/T_c)^2$. There is no abrupt discontinuity near T_c and the transition appears to be second order. This is as expected from a Landau theory of charge-density waves[14] for a normal to lock-in phase transition. The analog of the diffuse scattering in the electron diffraction pattern is seen here as a nonzero $(2a_0, 2c_0)$ intensity above background at the higher temperatures. Even at room temperature the $(2a_0, 2c_0)$ intensity is well above background.

We were able to measure the exact position of the superlattice below T_c and found that it was exactly commensurate within experimental error (2%). The position of the superlattice spots did not change with temperature.

III. RESISTIVITY AND MAGNETIC SUSCEPTIBILITY

Electrical resistivity measurements were also made on our crystals as a function of temperature both by a dc and an alternating-temperature technique. The shape and approximate magnitude of the results agree with those reported by Benda.[15] For example, the resistivity decreased with decreasing temperature but showed a noticeable plateau around 150 °K. This is probably due to formation of a gap over part of the Fermi surface or to phonon scattering. The phase transition is most

readily seen by the alternating temperature technique as shown in Fig. 3 where we plot differential resistivity $d\rho/dT$ vs T. The resistivity was of the order of magnitude 10^{-3} Ω cm at room temperature. Recent Hall measurements of similar $Ti_{1+x}Se_2$ crystals at 300 °K show a negative Hall effect and a mobility $\mu \sim 7$ cm²/V sec.[16] In a simple one carrier model these figures correspond to a carrier density $N = (1/\rho)/\mu e \sim 9 \times 10^{20}$ cm^{-3} or 0.06 electrons per molecule. This is reasonable but a little low for $x = 0.02$ since the excess titanium is known to enter between layers and thought to donate four electrons per atom. The discrepancy may be due to overlapping bands and the filling of hole states as indicated in Fig. 1.

The phase transition can also be studied by observing the magnetic susceptibility χ as a function of T. This was done by the Faraday technique using a Cahn microbalance and a superconducting solenoid capable of producing fields up to 60 kG. Sample temperature was carefully stabilized to ±1° using a control system and helium gas as a heat exchange fluid. About 100 mg of layer crystal were suspended in a basket oriented so that the magnetic field was perpendicular to the basal plane. Several runs were made on different crystals and typical results are shown in the lower part of Fig. 3. Because the susceptibility χ is very small and sample orientation critical, the absolute values of χ are uncertain. On the other hand, relative values are good to a few percent and the phase transition can be clearly seen. Different samples showed slightly different transition temperatures but the nonstoichiometric crystals reported on here had T_c in the range 145–160 °K.

It is possible to obtain useful information from the change in susceptibility $\Delta\chi$ just below T_c. This is done by assuming that below T_c a certain fraction f of the electrons close to the Fermi surface become ineffective in Pauli spin paramagnetism due to the formation of an energy gap associated with the $2a_0$ lattice distortion. The total susceptibility can be written as the sum of an orbital or diamagnetic part plus the Pauli electron contribution as follows:

$$\chi = \chi_{\text{orb}} + [\mu_B^2 S(E_F)/V][1 - f(1 - T^2/T_c^2)], \quad (1)$$

where μ_B is the Bohr magneton, $S(E_F)$ the density of states at the Fermi level, and V is the volume of the crystal. With reference to the sloping background shown by a dotted line in Fig. 3, the change in spin susceptibility (assumed isotropic) due to formation of a charge-density wave is

$$\Delta\chi = -(\mu_B^2 m/\pi\hbar^2 c_0) f(1 - T^2/T_c^2). \quad (2)$$

Here c_0 is the hexagonal axis lattice parameter, and we have substituted for the *two-dimensional* density of states $S = Am/\pi\hbar^2$, where A is the area of the crystal and the other quantities have their usual meaning. We now differentiate Eq. (2) with respect to temperature and compare with the observed data at $T = T_c$. The result is that $fm/m_0 = 0.19 \pm 0.05$, where m_0 is the free-electron mass. Thus if the electron effective mass is close to 1.0 (reasonable in comparison with band theory), a gap may form over as much as 20% of the Fermi surface!

The almost linear dependence of χ above T_c is difficult to understand. It does not appear to be an instrumental difficulty, although these are very small susceptibilities. The diamagnetic contribution to the first term in Eq. (1) depends upon the mean-square radial distribution of charge about the nuclei, and this should be only weakly temperature dependent. It is conceivable that this background is due to the fluctuations above T_c observed in the electron and x-ray diffraction. Notice that there is also a perceptable slope to this background in the x-ray scattering intensity of Fig. 3. It marks an instability or tendency toward superlattice formation as T_c is approached. The group-V*b* charge-density wave compounds studied so far are rather different in this regard. Further studies are underway, especially an investigation of the anisotropy of the overall susceptibility. See Note added in proof.

IV. INFRARED REFLECTIVITY

In an attempt to learn more about the carrier density and Fermi surface of $TiSe_2$ we undertook the measurement of reflectivity as a function of temperature in the infrared from 100 to 4000 cm^{-1}. The instruments used were a Beckman IR-11 and an IR-9 fitted with a beam concentrator-reflection attachment using nonspherical optics as described by Brandt.[17] Low-temperature measurements were made using a helium cryostat fitted with CsI and with polyethylene windows. Samples, including an aluminum reference mirror, could be rotated into the beam for near normal incidence reflection measurements without altering the path through the windows. Care was taken to avoid negative light effects when the sample was at low temperature. Freshly cleaved surfaces were prepared just before measurement or before establishing a vacuum. Wavelength resolution was of the order of 2 cm^{-1} and the uncertainty in reflectivity ±0.02.

Figure 4 shows the reflectivity of a $Ti_{1+x}Se_2$ ($x \sim 0.02$) crystal at room temperature and at 80 °K. The room-temperature curve agrees well with Lucovsky *et al.*[18] who have investigated similar crystals of $TiSe_2$, TiS_2, and the 1*T* tantalum compounds at room temperature. Notice that a heavily damped plasma reflectivity edge and minimum oc-

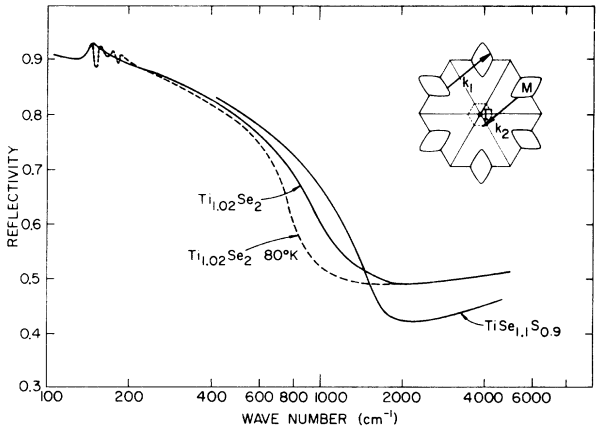

FIG. 4. Reflectivity of $Ti_{1+x}Se_2$ in the far infrared at room temperature and at 80 °K (dashed curve). Also shown is the observed reflectivity for a mixed crystal $TiSe_{1.1}S_{0.9}$ at room temperature. The inset shows the two-dimensional Brillouin zone for $1T$-$TiSe_2$ with occupied electron cylinders at M. Scattering wave vectors k_1 and k_2 are shown.

curs around 1000 cm^{-1}. In addition a feature appears in the room-temperature curve at 140 cm^{-1} which is probably due to phonons.

The dashed curve in Fig. 4 shows the observed reflectivity of the $Ti_{1+x}Se_2$ crystal cooled to about 80 °K. It can be seen that the 144 cm^{-1} feature has broken up into three or four bands. Maxima in reflectivity now appear at 140, 153, 175, and 199 cm^{-1}. Apparently there are additional infrared active modes in the smaller Brillouin zone associated with the superlattice. These matters will be discussed in a later publication.

When the $Ti_{1+x}Se_2$ crystal was slowly cooled toward liquid nitrogen the reflectivity around 900 cm^{-1} decreased noticeably. Two effects appeared the first being a more or less continuous change in the Drude edge which tracked the decreasing resistivity to liquid-helium temperature. The second component was of a different nature and accounted for most of the drop in reflectivity centered upon 800 cm^{-1} in Fig. 4. This part of the change began to set in abruptly upon cooling through the phase transition. Usually a conductivity or loss peak can be associated with a reflectivity change of this sort. Barker,[19] for example, has shown how an absorption peak appears in $2H$-$TaSe_2$ upon cooling through the charge density wave transition. In the case of $TiSe_2$ a complete separation of components and Kramers-Kronig analysis has not yet been done. The loss peak, however, occurs in the vicinity of 800 cm^{-1} or 0.1 eV. We suggest that this feature in the infrared reflectivity is due to a gap ($\sim 7kT_c$) opening up over part of the Fermi surface when the temperature falls below T_c.

Figure 4 also shows the Drude edge for a mixed crystal $TiSe_{1.1}S_{0.9}$ containing as much as 45% sulfur. This system was investigated in order to see the effect on the charge density waves and fluctuations. Notice that the plasmon edge has shifted very little suggesting carrier densities comparable to the pure selenides. It was found that the $2a_0$ superlattice transition was suppressed in the 45% sulfur crystal. The superlattice was found in dilute Se-S crystals but could not be observed above 120 °K when the sulfur concentration was 12% or more. Interestingly enough the diffuse streaking or $2a_0$ fluctuations of Fig. 1(a) were observed in mixed crystals containing as much as 75% sulfur.

V. CONCLUSIONS AND POSSIBLE MECHANISMS

We have thus made a variety of measurements on the interesting $(2a_0, 2c_0)$ superlattice which forms in slightly nonstoichiometric crystals of $TiSe_2$ at low temperature. Information on the temperature dependence of the order parameter was obtained from x-ray scattering. A second-order phase transition is found around $T_c = 150$ °K in the crystals studied. Both magnetic susceptibility and infrared reflectivity indicate that an energy gap begins to form at T_c over an appreciable part of the Fermi surface. Additional information is obtained from the far-infrared reflectivity data. For example, the 140-cm^{-1} lattice phonon feature[18] observed at room temperature breaks up into several bands upon cooling below T_c. These are consistent with the formation of a reduced Brillouin zone and a larger number of atoms per unit cell. Finally, fluctuations with strong diffuse scattering occurs above T_c and is readily observable to at least room temperature.

The transition temperature T_c does appear to vary somewhat from crystal to crystal probably due to slight differences in stoichiometry x. In fact, the transition can be suppressed by a large excess of titanium or by a high concentration of sulfur in the mixed crystals. On the other hand, the superlattice when it occurs appears to have an exactly $(2a_0, 2c_0)$ periodicity. The electronic properties, stoichiometry, etc., are important in connection with the transition strongly indicating that these are Fermi surface driven instabilities.

There are at least two possible models to explain these dominant and interesting features of $Ti_{1+x}Se_2$. The first model (i) involves the scattering of electrons from occupied states on the surface of one cylinder to unoccupied on another cylinder at M or L. The other model (ii) involves coupling between electrons at M (or L) and holes at Γ, as suggested by Wilson.[10] These two possibilities are shown schematically in the inset of Fig. 4 (where we have omitted the third dimension of the

Brillouin zone including the points at L). Suppose that the instability is due to strong intervalley (intercylinder) scattering as shown by k_1 in the upper part of the inset. Notice that it is possible to connect occupied states at the surface of one cylinder with unoccupied states at another surface by a wave vector k_1 which is in a principal direction and equal to a zone-boundary phonon wave vector. The cylinder cross sections sketched in Fig. 4 allow substantial "nesting" but other shapes are possible. If electron-phonon coupling is sufficiently strong, this could lead to soft-mode behavior and the $2a_0$ superlattice.

The acoustic-phonon spectrum of $TiSe_2$ has been recently measured by inelastic neutron scattering[20]; however the data do not extend to the zone boundary in the Γ to M or Γ to L directions. Clearly further neutron scattering work is called for, especially on the zone-boundary and optical modes.

In the more nearly stoichiometric crystals a hole surface will exist at the center of the zone Γ. Then it may be that electrons at M (or L) and holes at Γ are coupled as indicated by the wave vector k_2 in Fig. 4. Here the exact dependence of the phase transition (its occurrence and T_c) upon stoichiometry would be a deciding factor. It should be remarked that one would expect the charge-density wave to be commensurate with the lattice in both cases for reasons very much like those put forth by Herring in the case of the interaction between spin-density waves and the lattice.[21]

Note added in proof. The above analysis is only a first approximation. In recent work [J. Gaby *et al.* (to be published)] we find both the orbital and spin susceptibility anisotropic but the spin part to a lesser degree. An anisotropic spin susceptibility can probably be understood in terms of spin-orbit interaction.

ACKNOWLEDGMENTS

The authors would like to thank J. Wilson for early discussions on these materials. They also appreciate the help and comments of M. B. Salamon, M. Klein, and S. F. Meyer. Assistance by the electron microscope staff, especially I. D. Ward, and by the analytical group Judy Baker and J. Woodhouse is much appreciated.

---

*Research supported in part by the NSF under Grant No. DMR-72-03026.

[1]J. A. Wilson and A. Joffe, Adv. Phys. 18, 193 (1969).

[2]J. A. Wilson, F. J. DiSalvo, and S. Mahajan, Adv. Phys. 24, 117 (1975).

[3]H. W. Myron and A. J. Freeman, Phys. Rev. B 9, 481 (1974).

[4]L. F. Mattheiss, Phys. Rev. B 8, 3719 (1973).

[5]C. Riekel and R. Schollhorn, Mater. Res. Bull. 10, 629 (1975).

[6]A. H. Thompson, F. R. Gamble, and C. R. Symon, Mater. Res. Bull. 10, 915 (1975).

[7]B. Sonntag and F. C. Brown, Phys. Rev. B 10, 2300 (1974).

[8]Photoemission and appearance potential spectra also bear on this issue. See F. R. Shepherd and P. M. Williams, J. Phys. C 7, 4416 (1974); also C. Webb and P. M. Williams, Phys. Rev. B 11, 2082 (1975).

[9]R. Z. Bachrach, M. Skibowski, and F. C. Brown, Phys. Rev. Lett. 37, 40 (1976).

[10]A. H. Thompson, Phys. Rev. Lett. 34, 520 (1975).

[11]J. A. Wilson (private communication); F. J. DiSalvo, D. E. Moncton, and J. V. Waszczak, Phys. Rev. B (to be published).

[12]B. I. Halperin and T. M. Rice, Rev. Mod. Phys. 40, 755 (1968).

[13]H. Shafer, *Chemical Transport Reactions* (Academic, New York, 1964).

[14]W. L. McMillan, Phys. Rev. B 12, 1187 (1975).

[15]J. A. Benda, Phys. Rev. B 10, 1409 (1974).

[16]W. Stutius (private communication).

[17]R. C. Brandt, Appl. Opt. 8, 315 (1969).

[18]G. Lucovsky, W. Y. Liang, R. M. White, and K. R. Pisharody, Solid State Commun. 19, 303 (1976).

[19]A. S. Barker, Jr., J. A. Ditzenberger, and F. J. DiSalvo, Phys. Rev. B 12, 2049 (1975).

[20]W. G. Stirling, B. Dorner, J. D. N. Cheeke, and J. Revelli, Solid State Commun. 18, 931 (1976).

[21]C. Herring, in *Magnetism*, edited by G. T. Rado and H. Suhl (Academic, New York, 1966), Vol. IV, p. 340.

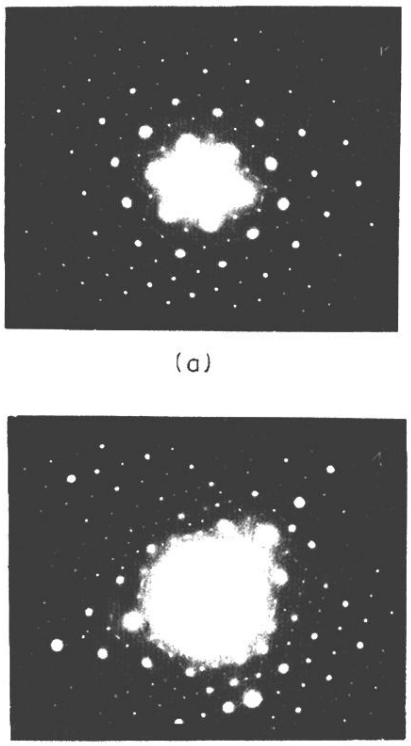

FIG. 2. (a) Electron diffraction pattern for a crystal of $Ti_{1+x}Se_2$ ($x \sim 0.02$) at room temperature. In addition to the normal hexagonal diffraction pattern diffuse streaking appears especially near the midpoints of the lines joining two spots. (b) A pattern for the same crystal at 120 °K which is below the lock-in transition. Note the sharp $\frac{1}{2}a_0^*$ spots.